

Biological synchronization and aggregation emerging from random processes

Jan Haškovec¹

Abstract. We present two individual based models where biological social phenomena emerge from purely random behavior of individuals, and there is no deterministic "social force" that would push the system towards its organized phase. Instead, organization on the global level results merely from reducing the individual noise level in response to local organization, which is induced by stochastic fluctuations. The first model describes the experimentally observed collective motion of locust nymphs marching in a ring-shaped arena and is written in terms of coupled velocity jump processes. The second model was inspired by observations of aggregative behavior of cockroaches in homogeneous environments and is based on randomly moving particles with individual diffusivities depending on the perceived average population density in their neighborhood. We show that both models have regimes with global self-organization (synchronization and aggregation). Moreover, we derive and study the mean-field limits for both models, leading to PDEs with nonlocal nonlinearities, and, in the second model, with possibly discontinuous coefficients.

1 Introduction

Collective behavior of large animal groups with self-organization (i.e., without the active role of a leader) into robust complex patterns is a fascinating natural phenomenon. Prominent examples are schools of fish or flocks of hundreds of starlings, who can fly as a uniformly moving group, as well as produce turbulent aerial displays. Apart from its biological and evolutionary relevance, collective phenomena play a prominent role in many other scientific disciplines, such as robotics, control theory, economics and social sciences, see, e.g., the recent surveys [4, 20].

Most of the standard models proposed in the literature are (or are derived from) individual based models (IBMs), where animals are modeled as particles following certain microscopic rules determined by their position and velocity inside the group and by the local density of conspecifics. These (typically simple) rules incorporate the "sociological" or "behavioral" components in animal movement, such as the social tendency to produce grouping (attraction/aggregation), the inherent minimal space they need to move without problems and feel comfortably inside the group (repulsion/collisional avoidance) and the mimetic adaptation or synchronization to a group (orientation/alignment). In the majority of established models of collective phenomena, such as [6, 9, 5], these rules are accounted for by deterministic terms. Noise, if present at all, typically has a "decorrelating" effect, i.e., works against the deterministic terms.

This paper offers an overview of two models of collective motion with a different modelling philosophy: On the individual level, they do not assume any deterministic "social force" that would push the system towards its organized phase. Instead, organization on the global level results merely from modulating the individual noise level in response to local organization, which is induced by stochastic fluctuations. Such approach is somehow novel in the area of mathematical modelling of collective motion. We will show that it is able to recover and possibly explain experimental observations and give an overview of the

¹Mathematical and Computer Sciences and Engineering Division, King Abdullah University of Science and Technology, Thuwal 23955-6900, Kingdom of Saudi Arabia; e-mail: jan.haskovec@kaust.edu.sa

mathematical analysis of the two models that follow this approach.

2 A velocity jump model for synchronization in locusts

Wingless desert locust nymphs form marching groups [2]. One of the most interesting aspects of the motion of these groups is their sudden coherent changes in direction. Buhl et al [2] studied an experimental setting, in which locust nymphs marched in a ring-shaped arena. At low densities there was a low incidence of alignment among individuals. Intermediate densities were characterized by long periods of collective motion in one direction along the arena interrupted by rapid changes of group direction. If the density of locusts was further increased, the group quickly adopted a common and persistent rotational direction.

In [7] a stochastic individual-based model of this experimental setting is formulated as a velocity jump process [18]. We consider a group of N agents (locusts) with time-dependent positions $x_i(t)$ and velocities $v_i(t)$, $i = 1, \dots, N$. To mimic the ring-shaped arena set-up of [2], we assume that the agents move along a one-dimensional circle, which we identify with the interval $\Omega = [0, 1)$ with periodic boundary conditions, and move either to the right or to the left with the same unit speed, i.e.

$$x_i(t) \in \Omega, \quad v_i \in \{-1, 1\} \quad \text{and} \quad \frac{dx_i}{dt}(t) = v_i(t). \quad (2.1)$$

We define the local average velocity of the ensemble, detected by the i -th agent, as

$$u_i^{loc} = \frac{\sum_{m=1}^N w(|x_i - x_m|) v_m}{\sum_{m=1}^N w(|x_i - x_m|)}, \quad (2.2)$$

where w is a bounded and nonnegative weight function defined on Ω . A typical choice is $w(s) = \chi_{[0, \sigma]}(s)$, where $\chi_{[0, \sigma]}$ is the characteristic function of the interval $[0, \sigma]$ and $\sigma > 0$ is a interaction radius.

The agents switch their velocities to the opposite direction based on N independent Poisson processes with the rates

$$\gamma_i = \gamma_0 + b(v_i - u_i^{loc})^2, \quad i = 1, \dots, N, \quad (2.3)$$

where $\gamma_0 \geq 0$ and $b \geq 0$ are fixed parameters. Obviously, the frequency of individual velocity jumps increases with a local or global loss of group alignment.

This velocity jump process describes the tendency of the individuals to align their velocities to the average velocity of their neighbors. Numerical simulations confirm that its predictions are in qualitative agreement with the experimental observations made in [2]: the transition to ordered motion as N grows (Figure 1) and the density-dependent switching behaviour between the ordered states (Figure 2, bottom).

Moreover, with the simplifying assumption $w \equiv 1$ in (2.2), i.e. $u_i^{loc} = u := \frac{1}{N} \sum_{i=1}^N v_i(t)$ for all $i = 1, \dots, N$, we obtain an explicit formula for the mean switching time between the two ordered states. Using Kramers theory [11, 10], the mean switching time can be approximated as

$$\tau_N(-u_s \mapsto u_s) \approx \frac{N\pi}{\gamma_0 + b} \frac{\exp(\Phi_N(0) - \Phi_N(-u_s))}{\sqrt{-\Phi_N''(0)\Phi_N''(-u_s)}}, \quad (2.4)$$

which has an exponential asymptotic with respect to large N given by

$$\tau_N(-u_s \mapsto u_s) \approx \frac{2\pi}{b - \gamma_0} \sqrt{\frac{\gamma_0}{2(\gamma_0 + b)}} \exp \left\{ N \left[\frac{b - \gamma_0}{2} - \frac{\gamma_0}{b} \ln \left(\frac{2\gamma_0}{\gamma_0 + b} \right) \right] \right\}.$$

This again is in agreement with the experimental observations, [2].

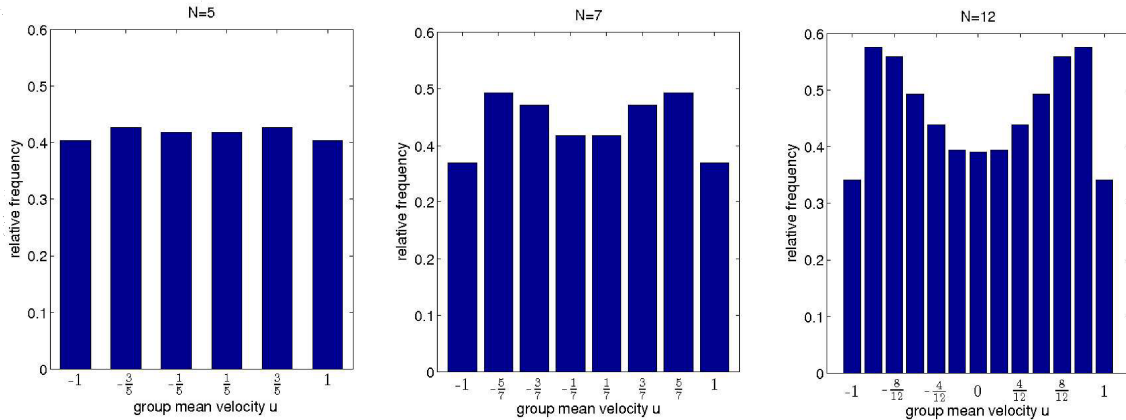


Figure 1: An example of the transition to ordered motion as N grows. We use (2.1)–(2.3) with $b = 1$, $\gamma_0 = 0.2$ and $w = \chi_{[0,0.2]}$. Shown are the normalized histograms of the group mean velocities $u = \frac{1}{N} \sum_{i=1}^N v_i$ recorded in 10^5 time steps of length 10^{-2} , with $N = 5$ (left panel), $N = 7$ (middle panel) and $N = 12$ individuals (right panel). The system does not prefer any particular state for $N = 5$. Two quasi-stable states of ordered collective motion are easily recognizable for $N = 12$.

2.1 Kinetic and hydrodynamic descriptions

Passing to the limit of large populations, $N \rightarrow \infty$ (see [7]), we obtain the kinetic system

$$\partial_t p^+ + \partial_x p^+ = -[\gamma_0 + b(1-u)^2]p^+ + [\gamma_0 + b(1+u)^2]p^-, \quad (2.5)$$

$$\partial_t p^- - \partial_x p^- = -[\gamma_0 + b(1+u)^2]p^- + [\gamma_0 + b(1-u)^2]p^+, \quad (2.6)$$

where $p^+(t, x)$ and, resp., $p^-(t, x)$, denote the densities of individuals marching to the right, and, resp., to the left, at time $t \geq 0$ and location $x \in \Omega$. The continuous analogue of the local average velocity (2.2) is given by

$$u(t, x) := \frac{\int_{\Omega} w(|x-z|)(p^+(t, z) - p^-(t, z)) dz}{\int_{\Omega} w(|x-z|)(p^+(t, z) + p^-(t, z)) dz} \quad \text{for } x \notin \mathcal{S}_0[p^+, p^-](t), \quad (2.7)$$

where

$$\mathcal{S}_0[p^+, p^-](t) := \left\{ x \in \Omega; \int_{\Omega} w(|x-z|)(p^+(t, z) + p^-(t, z)) dz = 0 \right\}.$$

The definition of $u(t, x)$ can be extended to the whole domain Ω by setting $u(t, x) = 0$ for $x \in \mathcal{S}_0[p^+, p^-](t)$, since u in (2.5)–(2.6) only appears in products with p^+ , p^- , which vanish on $\mathcal{S}_0[p^+, p^-](t)$.

Equivalently, defining the mass density ϱ and flux j by

$$\varrho(t, x) := p^+(t, x) + p^-(t, x), \quad j(t, x) := p^+(t, x) - p^-(t, x), \quad (2.8)$$

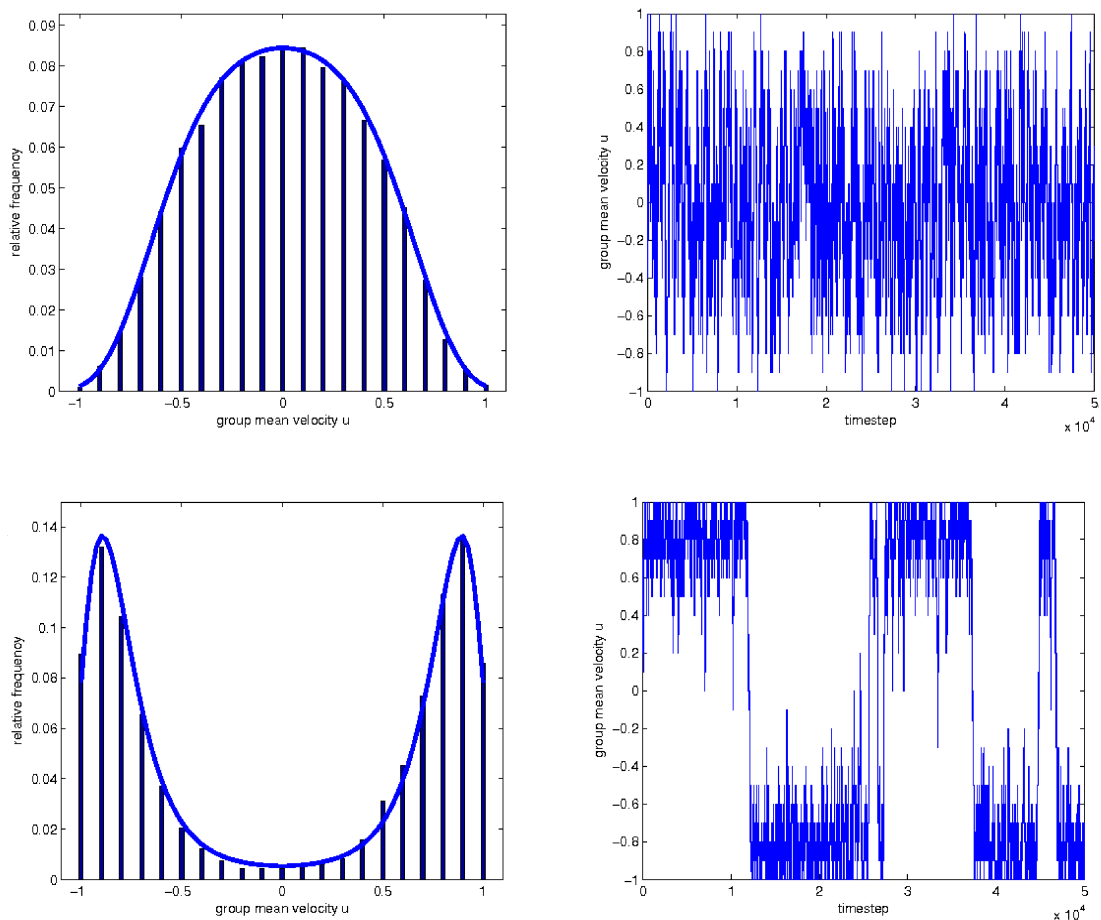


Figure 2: An example of the behaviour of the model (2.1)–(2.3) with global interactions ($w \equiv 1$): the large noise case (top) with $N = 20$, $b = 1$ and $\gamma_0 = 1.3$ and small noise case (bottom) with $N = 20$, $b = 1$ and $\gamma_0 = 0.3$. Left are the histograms of the group mean velocities u recorded in 10^5 time steps of length 10^{-2} , compared to the plot of the (properly scaled) stationary solution p_s of the corresponding Fokker-Planck equation (solid line). Right are the plots of the temporal evolution of the group mean velocity u during 5×10^4 timesteps. In the small noise case, one can clearly distinguish the two quasi-stationary states and observe the switching between them.

the system can be written in the hydrodynamic description as

$$\partial_t \varrho + \partial_x j = 0, \quad (2.9)$$

$$\partial_t j + \partial_x \varrho = -2[\gamma_0 + b(1 + u^2)]j + 4b\varrho u, \quad (2.10)$$

$$u(t, x) := \begin{cases} \frac{\int_{\Omega} w(|x-z|)j(t, z) dz}{\int_{\Omega} w(|x-z|)\varrho(t, z) dz}, & x \notin \mathcal{S}_0[\varrho](t), \\ 0, & x \in \mathcal{S}_0[\varrho](t), \end{cases} \quad (2.11)$$

with

$$\mathcal{S}_0[\varrho](t) := \left\{ x \in \Omega; \int_{\Omega} w(|x-z|)\varrho(t, z) dz = 0 \right\}.$$

In [7], the following Theorem regarding the existence of solutions to the above systems is proven:

Theorem 1 *For every $T > 0$ and every nonnegative initial datum $(p_0^+, p_0^-) \in L^\infty(\Omega) \times L^\infty(\Omega)$ there exists a nonnegative solution to the kinetic formulation (2.5)–(2.6) in $L^\infty([0, T] \times \Omega)$. This also establishes solutions $\varrho = p^+ + p^-$, $j = p^+ - p^-$ of the hydrodynamic formulation (2.9)–(2.11) with the corresponding initial condition.*

Moreover, analysis of the long time behavior of the above systems is possible in the particular case $w \equiv 1$, where $u(t, x) \equiv u(t)$ satisfies the ordinary differential equation (2.12) below. This ODE exhibits a pitchfork bifurcation, which is the classical picture for explaining ordering in models of Vicsek-Czirók type.

Lemma 1 *Assuming $w \equiv 1$, we have $u(t, x) \equiv u(t)$, where $u(t)$ satisfies the ordinary differential equation*

$$\dot{u} = -2(\gamma_0 + b(u^2 - 1))u, \quad (2.12)$$

subject to the initial condition $u(0) = \int_{\Omega} j(0, x) dx$. Moreover,

(i) *if $\gamma_0 \leq b$, then $\lim_{t \rightarrow \infty} u(t) = \text{sign}(u(0))\sqrt{1 - \gamma_0 b^{-1}}$,*

(ii) *if $\gamma_0 > b$, then $\lim_{t \rightarrow \infty} u(t) = 0$ and*

$$|u(t)| \leq |u(0)|e^{-2(\gamma_0 - b)t}. \quad (2.13)$$

Moreover, j converges to zero exponentially fast in the L^2 -sense:

$$\int_{\Omega} j^2(t, x) dx \leq ce^{-4\gamma_0 t}$$

for a suitable constant c .

Proof: See [7]. ■

Let us note that, formally, it is possible to consider even singular weights, in particular $w = \delta_0$, which leads to $u = j/\varrho$ and removes the nonlocality. In fact, one can see the choice $w = \delta_0$ as the limiting case when the interaction radius shrinks to zero: for almost all $x \in \Omega$ such that $\varrho(x) \neq 0$, one has

$$\lim_{\sigma \rightarrow 0} \frac{\int_{\Omega} \chi_{[0, \sigma]}(|x-z|)j(z) dz}{\int_{\Omega} \chi_{[0, \sigma]}(|x-z|)\varrho(z) dz} = \frac{j(x)}{\varrho(x)},$$

where $\chi_{[0, \sigma]}$ is the characteristic function of the interval $[0, \sigma]$. One can interpret this as a model where only pointwise local observations of the system are possible.

3 Individual based and mean-field modelling of direct aggregation in cockroaches

Animal aggregation is the process of finding a higher density of animals at some place compared to the overall mean density. Its formation may be triggered by some environmental heterogeneity that is attractive to animals, by physical currents that trap the organisms through turbulent phenomena, or by social interaction between animals [8, 17]. Aggregation may serve diverse functions such as reproduction, formation of local microclimates, anti-predator behaviour (see for instance [19] for a study of reducing the risk of predation to an individual by aggregation in *Aphis varians*), collective foraging and much more (see, e.g., [15] for a relatively recent survey). Aggregation also plays an important role as an evolutionary step towards social organization and collective behaviours [16]. These aspects explain the continuing interest in understanding not only the function of animal aggregation, but also the underlying mechanisms.

We introduce a model of biological aggregation based on randomly moving particles with individual stochasticity depending on the perceived average population density in their neighbourhood. The main novelty of this model is that we do not assume any explicit aggregative force acting on the individuals; instead, aggregation is obtained exclusively by modulating the amplitude of the individual random movement in response to perceived density of neighbors. This kind of behaviour was observed in insects, for instance the pre-social German cockroach *Blattella germanica*. In particular, the works by Jeanson et al. [13, 14] have shown that cockroach larvae aggregate in the absence of any environmental template or heterogeneity. In this case aggregation is the result of social interactions only and happens as a self-organized process.

In our model, the individuals are defined by their positions $x_i(t) \in \mathbb{R}^d$, $i = 1, \dots, N$, $d \geq 1$. Every individual is able to sense the average density of its close neighbors, given by

$$\vartheta_i(t) = \frac{1}{N} \sum_{j \neq i} W(x_i - x_j), \quad (3.1)$$

where $W(x) = w(|x|)$ with $w : \mathbb{R}^+ \rightarrow \mathbb{R}^+$ is a bounded, nonnegative and nonincreasing weight, integrable on \mathbb{R}^d . A generic example of w is the characteristic function of the interval $[0, R]$, corresponding to the sampling radius $R > 0$. The individual positions are subject to average density-dependent random walk,

$$dx_i = G(\vartheta_i) dB_i^t, \quad i = 1, \dots, N, \quad (3.2)$$

where B_i^t are independent d -dimensional Brownian motions and $G : \mathbb{R}^+ \rightarrow \mathbb{R}^+$ is a bounded, nonnegative and nonincreasing function. An example of the system dynamics with $G(s) = e^{-s}$ and $w(s) = \chi_{[0, R]}(s)$ and $N = 400$ particles is given in Fig. 3.

In [3] and we formally derived the mean-field limit of (3.1)–(3.2) as $N \rightarrow \infty$, which is the nonlinear diffusion equation for the particle density $\rho = \rho(t, x)$,

$$\frac{\partial \rho}{\partial t} = \frac{1}{2} \Delta_x (G(W * \rho)^2 \rho). \quad (3.3)$$

Global existence of weak solutions to (3.3) has been proved in [3], where even the degenerate case with $G(s) = 0$ for $s > s_0$ for some $s_0 > 0$ is allowed; in this case, however, only measure-valued (“very weak”)

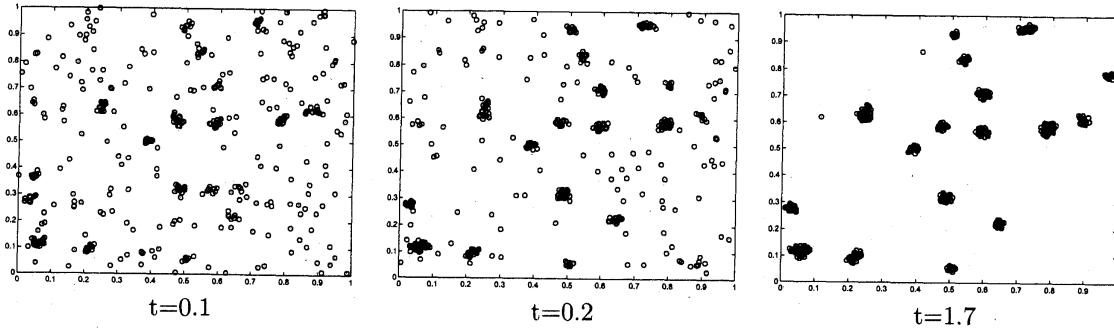


Figure 3: The individual based model (3.1)–(3.2) with $N = 400$ agents and sampling radius $R = 0.025$, subject to a random initial condition.

solutions exist. Linear stability analysis of constant steady states $\rho \equiv \rho_0$ can be done using the Fourier transform, and leads to the conclusion that those wavenumbers ξ of the perturbation are stable for which

$$\operatorname{Re} \hat{W}(\xi) < -\frac{G(\varrho_0)}{2G'(\varrho_0)\varrho_0} \geq 0,$$

where $\hat{W} = \hat{W}(\xi)$ is the Fourier transform of the kernel W . Since $W \in L^1(\mathbb{R}^d)$, we have $\hat{W} \in C^0(\mathbb{R}^d)$, and, therefore, all wavenumbers of $\tilde{\varrho}$ larger than a certain threshold will be stable. On the other hand, wavenumbers violating (3.4) will lead to pattern formation, as illustrated with the numerical example in Fig. 4.

Finally, in [12] we study the case when the response function G is discontinuous, in particular, it assumes two values only,

$$G(s) := \begin{cases} \overline{G} & \text{for } s \leq C, \\ \underline{G} & \text{for } s > C, \end{cases} \quad (3.4)$$

for some threshold $C > 0$. This is a model for a system with (constant) fast diffusion for low particle densities and slow diffusion for high particle densities. As shown in [12], it can be derived as a limit of a sequence of systems with smooth G . Typical patterns formed in the particle realization (3.1)–(3.2) with discontinuous G given by (3.4) is shown in Fig. 5, while the corresponding mean-field realizations subject to random initial data are shown in Figs. 6 and 7. These numerical simulations document the analytical result of [12] that stationary aggregation plateaus can only be either spherical, complements of sphericals or stripes. This can have biological consequences. In particular, the model can be used to describe P Granules in *C. elegans* embryos as protein aggregates and thus to model their condensation/decondensation which leads to their preferred localization in the posterior part of the cell upon symmetry breaking. This is motivated by the fact that P Granules have been shown to behave like droplike liquid phases that are in a dynamic equilibrium with soluble components within the cytoplasm [1].

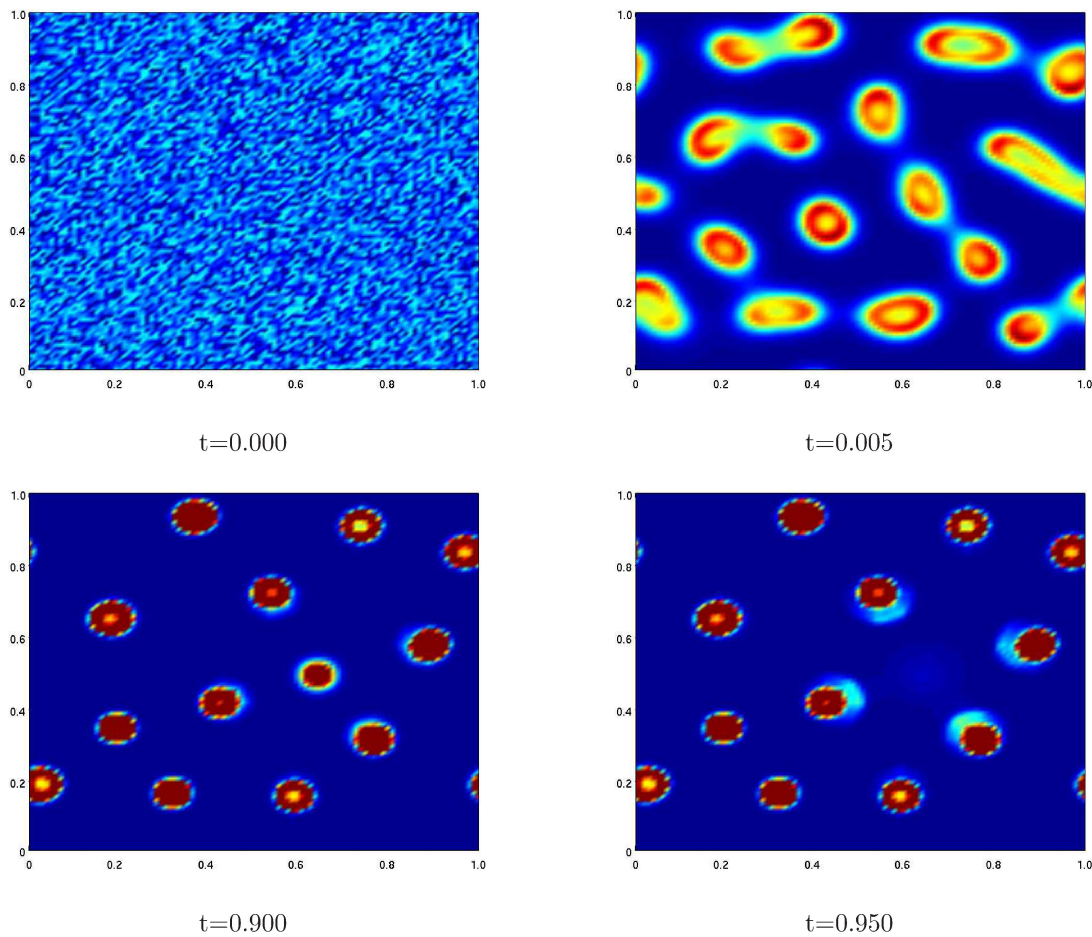


Figure 4: The first-order mean-field model in a periodic 2D setting with random initial condition (upper left panel). After the initial rapid smoothing of the high-frequency components, several ring-shaped structures are created (upper right panel), which eventually turn into an almost regular pattern of well localized aggregates (lower left panel). However, the smaller aggregates may be unstable and diffusively disintegrate, and their mass is absorbed by their neighbors, (lower right panel).

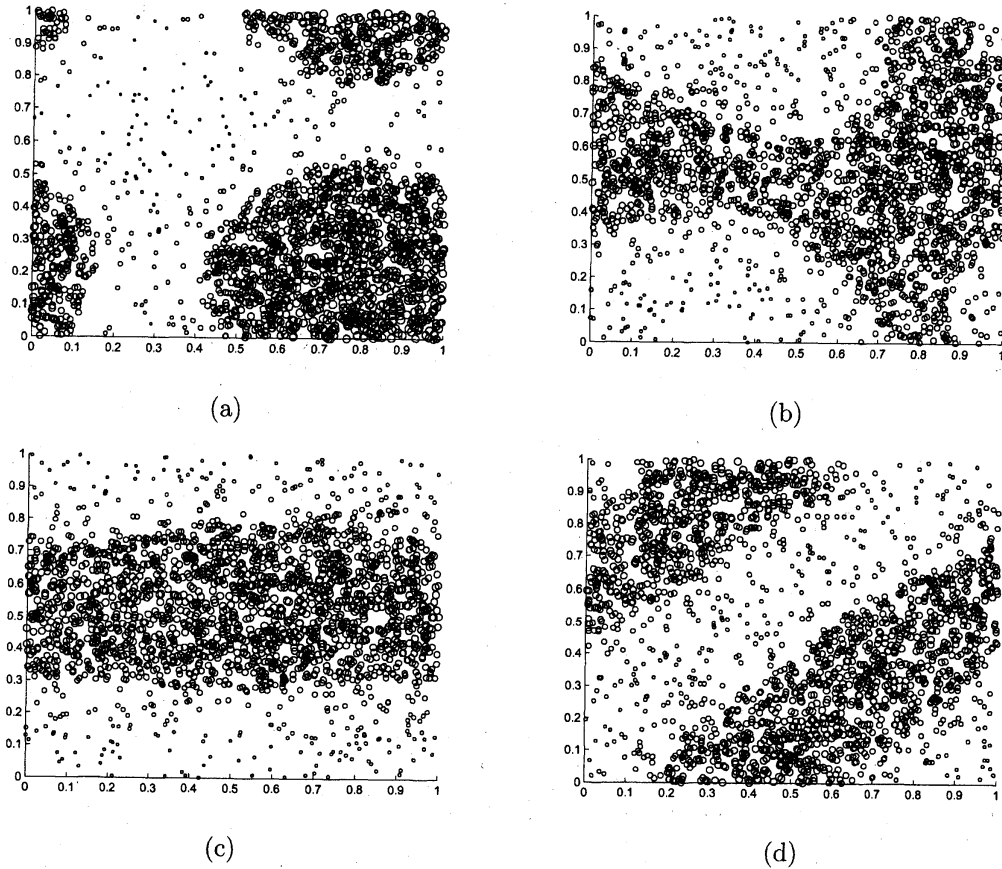


Figure 5: Typical patterns formed in different realizations of the stochastic individual based model (3.1)–(3.2) with the discontinuous response function G given by (3.4), with $N = 2000$ agents in the 2D domain $\Omega = [0, 1) \times [0, 1)$ with periodic boundary conditions, subject to a random initial condition. The size of the markers is proportional to the locally sensed density ϑ_i for each individual, given by (3.1).

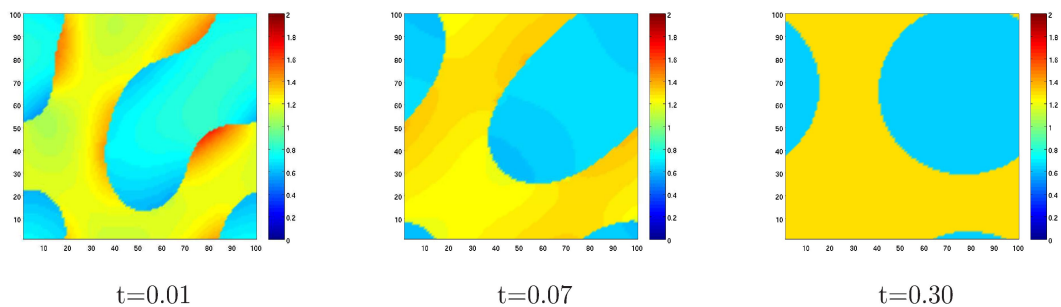


Figure 6: The 2D mean field model (3.3) with the discontinuous response function G given by (3.4) in a periodic 2D setting with random initial condition (not shown). In this realization a circular plateau has been formed in the steady state.

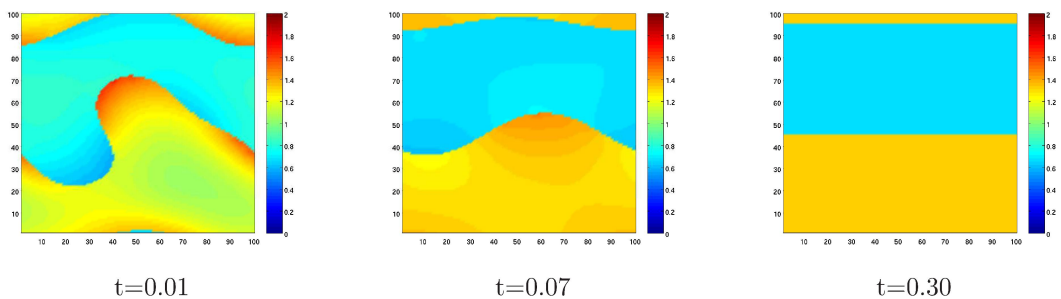


Figure 7: The 2D mean field model (3.3) in a periodic 2D setting with random initial condition (not shown). In this realization, a stripe-shaped plateau has been formed in the steady state.

References

- [1] C.P. Brangwynne, C.R. Eckmann, D.S. Courson, A. Rybarska, C. Hoege, J. Gharakhani, F. Jlicher, and A.A. Hyman: *Germline p granules are liquid droplets that localize by controlled dissolution/condensation*. Science **324** (2009), no. 5935, pp. 1729–1732.
- [2] J. Buhl, D. Sumpter, I. Couzin, J. Hale, E. Despland, E. Miller, and S. Simpson: *From disorder to order in marching locusts*. Science, **312** (2006), pp. 1402–1406.
- [3] M. Burger, J. Haskovec, and M.-T. Wolfram: *Individual-based and mean-field modelling of direct aggregation*. Physica D - Nonlinear Phenomena Vol. 260 (2012), pp. 145–158. doi: 10.1016/j.physd.2012.11.003.
- [4] J. Carrillo, M. Fornasier, G. Toscani, and F. Vecil: *Particle, kinetic, hydrodynamic models of swarming*, in “Mathematical Modeling of Collective Behavior in Socio-Economic and Life Sciences” (eds. G. Naldi, L. Pareschi, and G. Toscani), Modelling and Simulation in Science and Technology, Birkhäuser, (2010), pp. 297–336.
- [5] F. Cucker and S. Smale: *Emergent behavior in flocks*. IEEE Trans. Automat. Control **52** (2007), pp. 852–862.
- [6] A. Czirók, A. Barabási, and T. Vicsek: *Collective motion of self-propelled particles: Kinetic phase transition in one dimension*. Physical Review Letters, **82** (1999), pp. 209–212.
- [7] R. Erban and J. Haskovec: *From individual to collective behaviour of coupled velocity jump processes: a locust example*. Kinetic and Related Models Vol. 5, No. 4 (2012), pp. 817–842.
- [8] D. Grünbaum and A. Okubo: *Modelling social animal aggregations*. In: S. A. Levin (Ed.), Frontiers of Theoretical Biology. Vol. 100 of Lecture Notes in Biomathematics (1994), Springer-Verlag.
- [9] M. D’Orsogna, Y.-L. Chuang, A. Bertozzi and L. Chayes: *Self-propelled particles with soft-core interactions: patterns, stability, and collapse*. Phys. Rev. Lett. **96** (2006), pp. 104302–14.
- [10] D. Gillespie: *Markov Processes, an introduction for physical scientists*. Academic Press, Inc., Harcourt Brace Jovanowich, 1992.
- [11] P. Hänggi, P. Talkner, and M. Borkovec: *Reaction-rate theory: fifty years after Kramers*. Reviews of Modern Physics, **62** (1990), pp. 251–341.
- [12] J. Haskovec and D. Oelz: *A free boundary problem for aggregation by short range sensing and differentiated diffusion*. Preprint, 2013.
- [13] R. Jeanson, S. Blanco, R. Fournier, J.-L. Deneubourg, V. Fourcassié and G. Theraulaz: *A model of animal movements in a bounded space*. Journal of Theoretical Biology **225** (2003), pp. 443–451.
- [14] R. Jeanson, C. Rivault, J.-L. Deneubourg, S. Blanco, R. Fournier, C. Jost and G. Theraulaz: *Self-organised aggregation in cockroaches*. Animal Behaviour **69** (2005), pp. 169–180.
- [15] J. Krause and G. Ruxton: *Living in groups*. Oxford University Press, 2002.

- [16] J. Krebs and N. Davies (eds.): *Behavioural Ecology: An Evolutionary Approach*. Sinauer, Sunderland Massachusetts, 1984.
- [17] M. Mimura and M. Yamaguti: *Pattern formation in interacting and diffusing systems in population biology*. *Advances in Biophysics* 15 (1982), pp. 19–65.
- [18] H. Othmer, S. Dunbar, and W Alt: *Models of dispersal in biological systems*. *Journal of Mathematical Biology*, **26** (1988), pp. 263–298.
- [19] P. Turchin, P. Kareiva: *Aggregation in Aphis varians: an effective strategy for reducing predation risk*. *Ecology* 70 (1989), pp. 1008-1016.
- [20] T. Vicsek, A. Zafeiris: *Collective motion*. *Physics Reports* 517 (2012), pp. 71–140.